

# Magnetic Phase Diagram of Frustrated Spin Ladder

Takanori Sugimoto,<sup>1,\*</sup> Michiyasu Mori,<sup>2</sup> Takami Tohyama,<sup>1</sup> and Sadamichi Maekawa<sup>2</sup>

<sup>1</sup>*Department of Applied Physics, Tokyo University of Science, Katsushika, Tokyo 125-8585, Japan*

<sup>2</sup>*Advanced Science Research Center, Japan Atomic Energy Agency, Tokai, Ibaraki, 319-1195, Japan*

(Dated: June 19, 2019)

Frustrated spin ladders show magnetization plateaux depending on rung-exchange interaction and frustration defined by the ratio of first and second neighbor exchange interactions in each chain. This Letter is the first report on its magnetic phase diagram. Using the variational matrix-product state method, we accurately determine phase boundaries. Several kinds of magnetization plateaux are shown in the phase diagram. The frustration is necessary to obtain those plateaux, which are induced by strong correlation among quasi-particles on a lattice. Remarkable is that appropriate quasi-particles and their relevant interactions can be changed by a magnetic field. This will be useful to study many body physics as well.

Quantum phase transitions between spin liquid and magnetization-plateau (MP) phases are extensively studied in various low-dimensional spin systems with an interest of energy gaps emerging from spontaneously broken symmetry. These transitions are also the issue of correlated many-body systems and are closely related to the Mott transition in correlated electrons. According to the preceding studies [1–5], one of key factors is a commensurability energy of elementary excitations in spin systems. When the kinetic term is dominant as compared with the potential in an effective model, a spin liquid phase, i.e., metallic phase, is realized and its ground state is gapless. On the other hand, if the commensurability energy is relevant under a certain condition, the ground state can have a gap, and a MP phase, i.e., insulator phase, simultaneously appears. Oshikawa–Yamanaka–Affleck shows a condition for a magnetization per unit cell  $M$  to have the MPs [2, 4]. According to their argument, as increasing a commensurability energy (or potential energy) by introducing a perturbation competing against the kinetic energy, the system undergoes the gapless-to-gapped (spin-liquid-to-MP) transition, whose universality class is the same as the Berezinskii–Kosterlitz–Thouless (BKT) transition. To identify elementary excitations and to determine their effective models are the crucial points to study the spin-liquid-to-MP transition.

Previous studies on the two-leg spin ladder (2LSL) show that a quasi-particle different from spinon plays the role of elementary excitation in small-magnetization ( $M \sim 0$ ) and nearly-saturated ( $M \sim M_{\text{sat}}$ ) regions in the strong rung limit [6–11]. The quasi-particle at  $M \sim 0$  ( $M \sim M_{\text{sat}}$ ) is formed by a triplet (singlet) state on a rung, and is called triplon (singlon) as a hard-core boson [7]. The triplon (singlon) is a particle in a sea of rung singlets (triplets). It is noted that triplon and singlon can be associated with particle and hole, respectively. Since the chemical potential of the hard-core boson corresponds to a magnetic field, a half-filled band of hard-core bosons can be realized at a certain magnetic field giving  $M \sim M_{\text{sat}}/2$ . In this condition, instead of hard-core bosons, i.e., triplon and singlon, a quasi-spin

formed by the triplet and the singlet states well describes low-energy excitations around  $M \sim M_{\text{sat}}/2$  [9, 11]. Thus, it is important to choose an appropriate quantum object to describe magnetic excitations, and in the 2LSL our choice is changed by a magnetic field, i.e., magnetization.

Here, we switch on a frustration in a leg direction of 2LSL. The frustrated 2LSL (F-2LSL) has a gap in the ground state [10] and exhibits 1/3-, 1/2-, and 2/3-MP phases due to the competition between a frustration and the rung coupling [11]. Without rung coupling, we obtain two frustrated spin chains, which has a gap in its ground state and shows the 1/3-MP phase. It is explained by a boson-field model with a commensurability energy originating from the frustration [3, 12]. On the other hand, bosons with multiple components derived from the spin ladder have some types of interactions, whose commensurability energy originates from inter-chain couplings [4, 13]. These mechanisms of commensurability thus are different between chain and ladder. In short, the F-2LSL has various aspects in its character, i.e., frustrated spin chain and frustrated spin ladder. Therefore, a key factor of those MP phases is not obvious.

In this Letter, we show a magnetic phase diagram of the F-2LSL with respect to the frustration in each leg and the rung coupling. Using the variational matrix-product state (VMPS) method [14], each phase boundary can be accurately determined. Differences between triplon and singlon and between the 1/3- and 2/3-MP phases is discussed. At the same time, triplon-singlon correspondence based on the particle-hole symmetry of quasi-particles, is justified in the strong rung limit. Furthermore, characters of the quasi-particles in each phase are also shown. These characters are important for application of quantum magnets to spintronics such as spin Seebeck effect (SSE), which is a completely new method of thermoelectric generation [15, 16]. In fact, the SSE induced by spinons is different from that using usual ferromagnet [17].

We theoretically study magnetic phase diagram of F-

2LSL given by,

$$\mathcal{H} = \mathcal{H}_{\parallel} + \mathcal{H}_{\perp} + \mathcal{H}_Z, \quad (1)$$

with

$$\mathcal{H}_{\parallel} = \sum_{L=1,2} J_L \sum_j \sum_{i=u,1} \mathbf{S}_{j,i} \cdot \mathbf{S}_{j+L,i}, \quad (2)$$

$$\mathcal{H}_{\perp} = J_{\perp} \sum_j \mathbf{S}_{j,u} \cdot \mathbf{S}_{j,1}, \quad (3)$$

$$\mathcal{H}_Z = -H \sum_j \sum_{i=u,1} S_{j,i}^z. \quad (4)$$

There are three types of anti-ferromagnetic Heisenberg interactions: a nearest-neighbor coupling on a rung bond  $J_{\perp}$ , a nearest-neighbor coupling  $J_1$  and a next-nearest-neighbor coupling  $J_2$  in the leg direction. For simplicity, we introduce two rational angles, leg-rung ratio  $\alpha = \tan^{-1}(J_{\parallel}/J_{\perp})$  and frustration  $\beta = \tan^{-1}(J_2/J_1)$  with  $J_{\parallel} = \sqrt{J_1^2 + J_2^2}$ .

It is useful to note several limits and schematic picture of the MP states as discussed in Refs. [10, 11]. In the limit of weak rung coupling,  $J_{\perp} \ll J_1, J_2$  ( $\alpha \sim \pi/2$ ), this model approaches two decoupled frustrated spin chains, while a non-frustrated spin ladder is obtained in another limit of weak frustration,  $J_2 \ll J_1, J_{\perp}$  ( $\beta \sim 0$ ). This model (1) bridges between the frustrated spin chains and the non-frustrated spin ladder through  $J_{\perp}$  and  $J_2$ . This nature appears also in zero magnetic field as two different phases: columnar-dimer and rung-singlet phases. In the columnar-dimer phase, the ground state is composed of two degenerated states with spontaneously-broken translational symmetry [12], while the rung-singlet phase has no degeneracy in its ground state.

The nature bridging two different systems is more apparent in the MP states with finite magnetizations. For instance, the 1/2-MP phase is not allowed in the weak rung limit, because a frustrated spin chain does not exhibit a 1/2-MP phase. However, it becomes possible in the strong rung limit with a frustration, because the effective Hamiltonian around 1/2-MP corresponds to a frustrated quasi-spin chain with an effective magnetic field given by [11],

$$\mathcal{H}_{\text{eff}}^{(1)} = \mathcal{P}\mathcal{H}\mathcal{P} = \mathcal{H}'_{\parallel} + \mathcal{H}'_Z \quad (5)$$

with

$$\mathcal{H}'_{\parallel} = \sum_{\eta=1,2} \sum_j \left[ J_{\eta}^{z'} T_j^z T_{j+\eta}^z + J_{\eta}^{x'} (T_j^x T_{j+\eta}^x + T_j^y T_{j+\eta}^y) \right] \quad (6)$$

$$\mathcal{H}'_Z = -H' \sum_j T_j^z, \quad (7)$$

where  $\mathcal{P}$  is a projection operator, which projects out two of rung triplets as irrelevant high-energy states, and  $\mathbf{T}_j$  is the quasi-spin operator at  $j$ th rung composed by singlet

and triplet states on a rung (see Sec. I in Supplemental material for the detailed derivation [18]). The XY- and Ising-components of effective exchange interactions are denoted by  $J_{\eta}^{x'} = J_{\eta}$  and  $J_{\eta}^{z'} = J_{\eta}/2$  with  $\eta = 1, 2$ , respectively. In this picture, relationship between the quasi-spin magnetization  $M'$  and the real magnetization  $M$  is given by  $M'/M'_{\text{sat}} = 2M/M_{\text{sat}} - 1$ , so that the 1/2-MP state is regarded as the quasi-spin dimer state in the Majumdar-Gosh Hamiltonian [12]. Additionally, this picture in the strong rung limit derives other MPs, namely 1/3- and 2/3-MP states, which correspond to  $\mp 1/3$ -MP states in terms of quasi-spins respectively, as discussed in several spin- $\frac{1}{2}$  chains [19, 20]. In the weak rung limit, however, there does not appear 2/3-MP state, but only 1/3-MP state does. Therefore, we expect that a difference between the triplet and singlet states will be enhanced as decreasing the rung interaction from the strong rung limit. This is a kind of particle-hole symmetry breaking of hard-core quasi-particles.

To clarify phase boundaries of the MP states, we apply the VMPS method [14] to calculate the ground-state energies  $E_M(N)$  with finite magnetization  $M$  in finite system size  $N$ . The MP gaps  $\Delta_M$  are obtained as extrapolated values of  $E_{M+1}(N) + E_{M-1}(N) - 2E_M(N)$  with respect to inverse system size  $1/N \rightarrow 0$ . The ground-state energies  $E_M(N)$  are calculated up to  $N = 288$  spins with keeping the number of states  $m = 1000$  at most. The phase boundaries are determined as points at which the MP gap turns from positive to zero (or negative) with respect to the control parameter in Fig. 1 (see Sec. II in Supplemental material for the setup of numerical calculations and an example [18]).

Figure 1 shows the magnetic phase diagram with several MP phases. In Fig. 1(a), possible regions of MP phases at each  $M$  are shown with respect to rung interactions and frustration, which are parametrized by  $\alpha$  and  $\beta$ , respectively. The four figures in Fig. 1(a) are mapped into one plane as shown in Fig. 1(b). Firstly, we can confirm a coincidence of the phase boundaries of 1/3- and 2/3-MP phases in the strong rung limit [ $\alpha \rightarrow +0$  in Fig. 1(b)]. This coincidence can be explained well in quasi-spin effective Hamiltonian, because these MP states correspond to negative and positive 1/3-MP states in terms of quasi-spins as mentioned above. The coincidence, however, is broken by a small intra-chain interaction, especially for the upper boundaries. This discrepancy is more emphasized as increasing intra-chain interactions ( $\alpha \rightarrow \pi/2$ ), and at last, 2/3-MP state disappears, though 1/3-MP state can survive. The disappearance of 2/3-MP state is the consequence of the frustrated spin chain involved in the F-2LSL. We can also confirm a boundary between chain and ladder by the rung parity  $P_{\text{rung}} = \prod_j (2\mathbf{S}_{j,u} \cdot \mathbf{S}_{j,1} + \frac{1}{2}) = \pm 1$  and degeneracy of the ground states for 1/3-MP phase. This is because the 1/3-MP state in the weak rung limit ( $\alpha \rightarrow \pi/2$ ) is two frus-

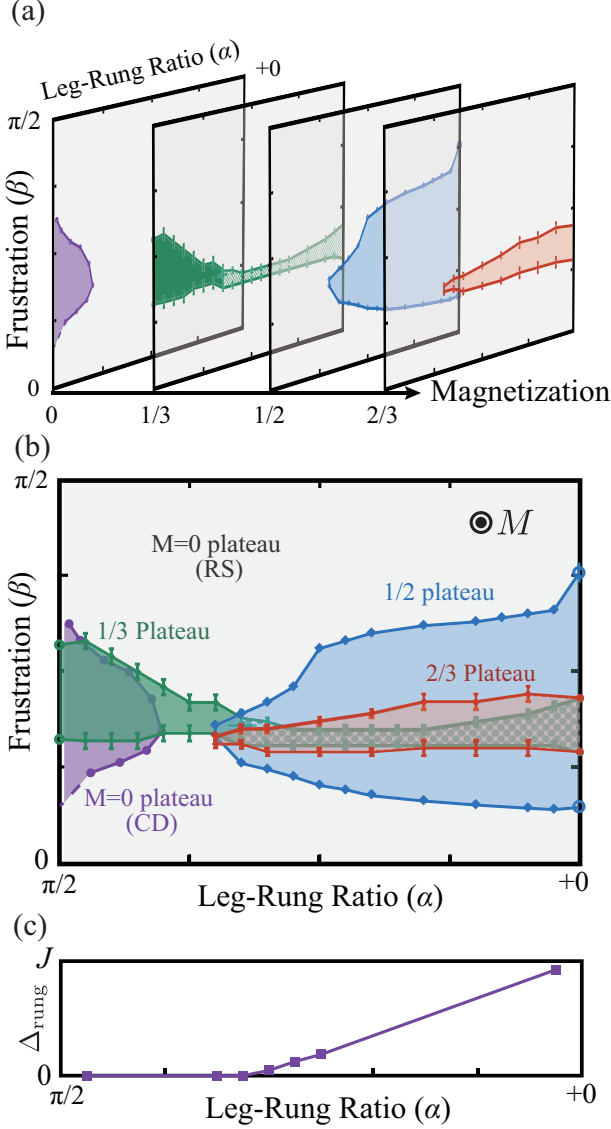


FIG. 1. (a) Magnetic phase diagrams and (b) comparison of the phase diagrams of F-2LSL, where the boundary of  $M = 0$  plateau phases, columnar dimer (CD) and rung singlet (RS), is referenced by Ref. [10]. In these diagrams, uncolored (gray) regions denote the gapless phases, except for  $M = 0$ . (c) Energy gap  $\Delta_{\text{rung}}$  as a function of  $\alpha$ , which indicates a gap opening behavior at a critical point  $\alpha_c \cong 0.350\pi$  in 1/3-magnetized ground states. This point corresponds to the boundary between the green and shaded green regions in Figs. (a) and (b).

trated spin chains, which is different from the strong rung limit ( $\alpha \rightarrow +0$ ). The ground state of two frustrated spin chains has two-fold degeneracy in terms of  $P_{\text{rung}} = \pm 1$ , while there is no degeneracy in the strong rung limit and the parity is given by  $P_{\text{rung}} = (-1)^{2N/3}$  with 1/3 magnetization in a  $N$ -rung system where the triplet (singlet) state with the rung parity  $+1$  ( $-1$ ) occupies  $N/3$  ( $2N/3$ ) rungs. Figure 1 (c) shows a gap  $\Delta_{\text{rung}}$ , which is defined as an energy gap between the  $P_{\text{rung}} = \pm 1$  ground states

with 1/3 magnetization. This is obtained by the VMPS method with an auxiliary field  $\mu|P_{\text{rung}} \pm 1|$  [21]. We can see that the gap  $\Delta_{\text{rung}}$  opens at  $\alpha \sim 0.325\pi$  as increasing rung coupling (decreasing  $\alpha$ ) at the 1/3-MP state. This boundary of two different 1/3-MP phases gives a good correspondence to the critical point ( $\alpha \sim 0.350\pi$ ) where the 2/3-MP phase disappears as decreasing  $\alpha$ . Moreover, the critical point of 1/2-MP phases is interestingly close to the boundary, so that the boundary intuitively indicates a crossover between two different models, namely chain and ladder.

Based on the discussion above, in the smaller  $\alpha$  region than the boundary ( $\alpha \lesssim \frac{3}{8}\pi$ ), the quasi-spin picture should work well. To explain the discrepancy between the 1/3- and 2/3-MP phases in this region, we consider higher-order approximation of the original Hamiltonian as follows,

$$\mathcal{H}_{\text{eff}}^{(2)} = \mathcal{P}\mathcal{V}(E_0 - \mathcal{H}_{\perp} - \mathcal{H}_Z)^{-1}\mathcal{Q}\mathcal{H}_{\parallel}\mathcal{P} = \mathcal{H}_{\text{eff}}^{(2a)} + \mathcal{H}_{\text{eff}}^{(2b)}, \quad (8)$$

where  $\mathcal{Q}$  is an orthocomplemental projection of  $\mathcal{P}$  and we use the unperturbed ground-state energy as an approximated eigen-energy [18]. As a second-order term of effective Hamiltonian, we find a symmetry-breaking term of quasi-spin inversion ( $T_j^z \rightarrow -T_j^z$ ,  $T_j^+ \rightarrow T_j^-$ , and its Hermite conjugate) given by,

$$\begin{aligned} \mathcal{H}_{\text{eff}}^{(2a)} = & - \sum_j \left[ \sum_{L=1,2} J_L'' (T_j^+ T_{j+2L}^- + T_j^- T_{j+2L}^+) T_{j+L}^z \right. \\ & \left. + J'' (T_j^+ T_{j+3}^- + T_j^- T_{j+3}^+) (T_{j+1}^z + T_{j+2}^z) \right] \quad (9) \end{aligned}$$

The other term  $\mathcal{H}_{\text{eff}}^{(2b)}$  has the same form as the first-order Hamiltonian. By the quasi-spin inversion, the Hamiltonian  $\mathcal{H}_{\text{eff}}^{(2a)}$  changes the sign. In these terms, the second-neighbor hopping with an intermediate-site magnetization, i.e., the first term of  $\mathcal{H}_{\text{eff}}^{(2a)}$ , can affect the second-neighbor hopping of the first-order Hamiltonian, so that this term can change the BKT transition point. To clarify an effect of the first term in (9), we consider the mean-field Hamiltonian given by,

$$H_{\text{MF}} \cong -J_1'' \bar{T}^z \sum_j (T_j^+ T_{j+2}^- + T_j^- T_{j+2}^+) - 2J_1'' \chi_1 \sum_j T_j^z, \quad (10)$$

where  $\bar{T}^z = \sum_j \langle T_j^z \rangle / N$  and  $\chi_1 = \sum_j \Re \langle T_{j-1}^+ T_{j+1}^- \rangle / N$ . The second term changes the critical magnetic field, at which the MP state appears. Since  $\bar{T}^z$  changes the sign from negative to positive at the half filling, the first term turns from additive to subtractive to the second-neighbor hopping, as increasing the magnetization. In particular, the second-neighbor interaction dominates around the upper boundaries of the 1/3- and 2/3-MP states as compared with the first-neighbor interaction. Here, a large hopping interaction suppresses the MP gap and thus, this term affects the MP boundaries as follows: the upper boundary of the 1/3-MP phase slides down with a help of this term, but that of the 2/3 slides up.

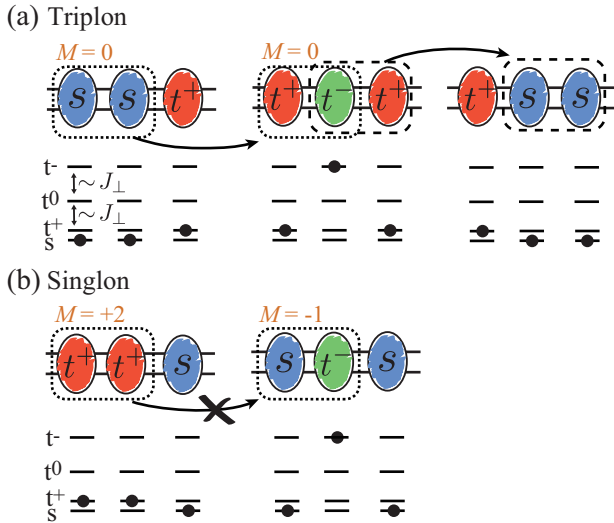


FIG. 2. Schematic difference of the second-order term of the effective Hamiltonian (9) between (a) triplon and (b) singlon. Colored ovals including a character  $s$  ( $t^\pm$ ) denote the singlet (triplet) states of rung. The energy levels of each rung, i.e., the singlet  $s$  and triplets  $t^{\pm,0}$ , are shown as solid lines below the oval, and the occupied state is represented by a black dot. In the small-magnetization (nearly-saturated) region with a strong rung interaction, the triplet (singlet) state behaves as a hard-core boson, which is called triplon (singlon), in the sea of singlets (triplets). A perturbative leg interaction does allow pair annihilation (dotted-lined area) and creation (dashed-lined area) of singlet in (a), but prohibit those of triplet in (b), because of the conservation law of magnetization  $M$ . In (a), we can see triplon hopping to the 2nd neighboring rung, through the intermediate state with an occupation of high energy levels.

The quasi-spin picture can correspond to the quasi-particle picture in small-magnetization region as triplons or nearly-saturated region as singlons. From the quasi-particle point of view, the asymmetric term results in difference of kinetic energy (see Fig. 2). In small-magnetization region [Fig. 2(a)], a small leg interaction can create and annihilate a singlet pair by using a neighboring triplet pair of opposite magnetizations  $M = \pm 1$  as keeping the conservation law of magnetization, where triplet with negative magnetization ( $t^-$ ) has a much higher energy than those of a triplet state ( $t^+$ ) and a singlet state ( $s$ ) and plays the role of an intermediate state. On the other hand, in nearly-saturated region [Fig. 2(b)], a leg perturbation cannot create and annihilate a triplet pair of the same magnetization  $M = +1$  by using any other two rung states, because two rung states with the magnetization  $M = +2$  are unique.

In fact, suppose a non-interacting case, higher-order long-ranged hopping terms renormalize the velocity of hard-core boson,  $v_0 = \partial \epsilon_k / \partial k \sim k \sum_{L=1,2,\dots} L^2 t_L = t' k$  around the minimum energy in the dispersion relation  $\epsilon_k = -\sum_L t_L \cos(Lk)$ , where  $t_L$  is  $L$ th neighbor hopping

obtained as higher-order approximation of  $J^x$ s and  $t'$  is a renormalized hopping. Thus, the kinetic energy of quasi-particle in small-magnetization region is relatively larger than that in nearly-saturated region.

In summary, we determined the magnetic phase diagram of the frustrated two-leg spin ladder by using the VMPS method. We found the 1/3-, 1/2-, and 2/3-MP phases in the diagram with respect to the frustration and the inter-chain interaction. All MPs are suppressed around one point ( $\alpha \sim \frac{3}{8}\pi$  and  $\beta \sim \frac{3}{16}\pi$ ) in the phase diagram. This shows crossovers between chain and ladder, and between frustrated and not frustrated systems. Furthermore, the difference between singlet- and triplet-based quasi-particles is clarified even with a small leg interaction. This difference originates from the second-order perturbation of leg interaction, which implies the kinetic energy of quasi-particle in small-magnetization region is larger than that in nearly-saturated region. The quasi-particles, triplon and singlon, are elementary excitations not only in ladder systems such as  $\text{BiCu}_2\text{PO}_6$  [22–27], but also strong dimer models such as two-dimensional Shastry-Sutherland compound  $\text{SrCu}_2(\text{BO}_3)_2$  [28] and three-dimensional spin-dimer compound  $\text{TlCuCl}_3$  [29]. Thus, our results on the quasi-particles will lead to a general concept of those materials.

Our results will be useful also for spin transport and spin current generation [15–17]. For example, electrical signals can be transmitted by magnons in a magnetic insulator [30]. Since the spin current carried by those magnons do not have Joule heat, magnon in a magnetic insulator is an idealistic choice to replace an electron's spin. In general, however, a magnetic field leads to a gap in a magnon's dispersion relation and suppresses a magnon distribution in low energies. This disadvantage will be compensated by the triplon, since it is stabilized in a magnetic field and has a well defined dispersion relation [11]. In addition to this, the triplon and the singlon in the F-2LSL play the role of particle and hole in a semiconductor, and hence will have another possibility of logic device, data storage, and information processing.

We would like to thank M. Fujita and O. P. Sushkov for valuable discussions. This work was partly supported by Grant-in-Aid for Scientific Research (Grant No.25287094, No.26103006, No.26108716, No.26247063, No.26287079, No.15H03553, and No.15K05192), Grants-in-Aids for Young Scientists (B) (Grant No.16K17753), and the inter-university cooperative research program of IMR, Tohoku University. Numerical computation in this work was carried out on the supercomputers at JAEA and the Supercomputer Center at Institute for Solid State Physics, University of Tokyo.

- 
- \* sugimoto.takanori@rs.tus.ac.jp
- [1] E. H. Lieb, T. Schultz, and D. J. Mattis, *Ann. Phys. (N.Y.)* **16**, 407 (1961);
- [2] M. Oshikawa, M. Yamanaka, and I. Affleck, *Phys. Rev. Lett.* **78**, 1984 (1997).
- [3] F. D. M. Haldane, *Phys. Rev. B* **25**, 4925 (1982); **26**, 5257(E) (1982).
- [4] K. Totsuka, *Phys. Rev. B* **57**, 3454 (1998).
- [5] M. Oshikawa, *Phys. Rev. Lett.* **90**, 236401 (2003).
- [6] As a review, E. Dagotto and T. M. Rice, *Science* **271**, 618 (1996).
- [7] S. Gopalan, T. M. Rice, and M. Sigrist, *Phys. Rev. B* **49**, 8901 (1994).
- [8] O.P. Sushkov and V.N. Kotov, *Phys. Rev. Lett.* **81**, 1941 (1998).
- [9] T. Giamarchi and A. M. Tsvelik, *Phys. Rev. B* **59**, 11398 (1999).
- [10] A. Lavaré, G. Roux, and N. Laflorencie, *Phys. Rev. B* **84**, 144407 (2011).
- [11] T. Sugimoto, M. Mori, T. Tohyama, and S. Maekawa, *Phys. Rev. B* **92**, 125114 (2015).
- [12] C. K. Majumdar and D. K. Ghosh, *J. Math. Phys.* **10**, 1399 (1969).
- [13] A. A. Nersisyan, A. O. Gogolin, and F. H. L. Eßler, *Phys. Rev. Lett.* **81**, 910 (1998).
- [14] For example, see U. Schollwöck, *Annal. Phys.* **326**, 965 (2011)
- [15] K. Uchida, S. Takahashi, K. Harii, J. Ieda, W. Koshibae, K. Ando, S. Maekawa and E. Saitoh, *Nature* **455**, 778 (2008)
- [16] H. Adachi, K. Uchida, E. Saitoh, and S. Maekawa, *Rep. Prog. Phys.* **76**, 036501 (2013). References therein.
- [17] D. Hirobe, M. Sato, T. Kawamata, Y. Shiomi, K. Uchida, R. Iguchi, Y. Koike, S. Maekawa, and E. Saitoh, *Nature Physics* **13**, 30 (2017).
- [18] See Supplemental Material at [http://link.aps.org/\\*\\*](http://link.aps.org/**).
- [19] K. Hida, *J. Phys. Soc. Jpn.* **63**, 2359 (1994).
- [20] K. Okunishi and T. Tonegawa, *J. Phys. Soc. Jpn.* **72**, 479 (2003); *Phys. Rev. B* **68**, 224422 (2003).
- [21] In this calculation, it is not necessary to target  $P_{\text{rung}}|G.S.\rangle$  in addition to  $|G.S.\rangle$  in the case of  $[P_{\text{rung}}, \mathcal{H}] = 0$ , because  $P_{\text{rung}}|G.S.\rangle = \pm|G.S.\rangle$ .
- [22] A. A. Tsirlin, I. Rousochatzakis, D. Kasinathan, O. Janson, R. Nath, F. Weickert, C. Geibel, A. M. Lauchli, and H. Rosner, *Phys. Rev. B* **82**, 144426 (2010).
- [23] Y. Kohama, S. Wang, A. Uchida, K. Prsa, S. Zvyagin, Y. Skourski, R. D. McDonald, L. Balicas, H. M. Ronnow, C. Rüegg, and M. Jaime, *Phys. Rev. Lett.* **109**, 167204 (2012).
- [24] L. Splinter, N. A. Drescher, H. Krull, and G. S. Uhrig, *Phys. Rev. B* **94**, 155115 (2016).
- [25] K. Hwang and Y. B. Kim, *Phys. Rev. B* **93**, 235130 (2016).
- [26] K. W. Plumb, K. Hwang, Y. Qiu, L. W. Harriger, G. E. Granroth, A. I. Kolesnikov, G. J. Shu, F.C. Chou, Ch. Rüegg, Y. B. Kim, and Y.-J. Kim, *Nat. Phys.* **12**, 224 (2016).
- [27] Regarding  $\text{BiCu}_2\text{PO}_6$ , we need to consider the Dzyaloshinskii-Moriya interaction, although most of our results will be satisfied qualitatively.
- [28] K. Kodama, M. Takigawa, M. Horvatić, C. Berthier, H. Kageyama, Y. Ueda, S. Miyahara, F. Becca, and F. Mila, *Science* **298**, 395 (2002).
- [29] Ch. Rüegg, N. Cavadini, A. Furrer, H.-U. Güdel, K. Krämer, H. Mutka, A. Wildes, K. Habicht and P. Vorderwisch, *Nature* **423**, 62 (2003).
- [30] Y. Kajiwar, K. Harii, S. Takahashi, J. Ohe, K. Uchida, M. Mizuguchi, H. Umezawa, H. Kawai, K. Ando, K. Takanashi, S. Maekawa, and E. Saitoh, *Nature* **464**, 262 (2010).